ISSN: 2581-5989
PubMed - National Library of Medicine - ID: 101738774

International Journal of Dental Science and Innovative Research (IJDSIR)

IJDSIR : Dental Publication Service

Available Online at:www.ijdsir.com

Volume – 9, Issue – 2, March – 2026, Page No. : 80 – 99

Comparative Analysis of Stress Distribution on Implant Supported Mandibular Prostheses Using Three Different Framework Materials- A Three-Dimensional Finite Element Analysis

[1]Dr. Vaishali Kalra, Senior Resident, Department of Prosthodontics, Bhojia Dental College and Hospital, Baddi, Himachal Pradesh, India

[2]Dr. Tarun Kalra, Professor and Head, Department of Prosthodontics, Bhojia Dental College and Hospital, Baddi, Himachal Pradesh, India

[3]Dr. Manjit Kumar, MDS, Professor, Department of Prosthodontics, Bhojia Dental College and Hospital, Baddi, Himachal Pradesh, India

[4]Dr. Ajay Bansal, Professor, Department of Prosthodontics, Bhojia Dental College and Hospital, Baddi, Himachal Pradesh, India

[5]Dr. Abhishek Avasthi, Professor, Department of Prosthodontics, Bhojia Dental College and Hospital, Baddi, Himachal Pradesh, India

[6]Dr. Arpit Sikri, Professor, Department of Prosthodontics, Bhojia Dental College and Hospital, Baddi, Himachal Pradesh, India

Corresponding Author: Dr. Manjit Kumar, MDS, Professor, Department of Prosthodontics, Bhojia Dental College and Hospital, Baddi, Himachal Pradesh, India

Citation of this Article: Dr. Vaishali Kalra, Dr. Tarun Kalra, Dr. Manjit Kumar, Dr. Ajay Bansal, Dr. Abhishek Avasthi, Dr. Arpit Sikri, "Comparative Analysis of Stress Distribution on Implant Supported Mandibular Prostheses Using Three Different Framework Materials- A Three-Dimensional Finite Element Analysis", IJDSIR- March – 2026, Volume – 9, Issue – 2, P. No. 80 – 99.

Type of Publication: Original Research Article

Conflicts of Interest: Nil

Abstract

Aim and Objectives: This study aimed to assess how stress is distributed in mandibular prostheses supported by implants with Titanium, Zirconia, and Cobalt-Chromium frameworks. The objective was to evaluate and compare the stress distribution among these three framework materials in implant-supported mandibular prostheses.

Materials and Method: Three implant-supported prostheses were modeled and divided into three infrastructure materials: Titanium, Zirconia, and Cobalt-Chromium. These bars were then attached to the modeled mandible. An axial load of 200 N was applied to a standardized area for all the systems. Maximum Von Mises stress generated in cortical bone, cancellous bone,

implant, implant screw, and the metal structure was analyzed using finite element analysis.

Results: The study found that maximum Von Mises stress in cortical and cancellous bone was slightly higher in Titanium compared to Zirconia and Cobalt-Chromium frameworks. Stress on the implant and metal structure was similar across all three materials; however, Zirconia and Cobalt-Chromium frameworks showed slightly higher stress on implant screws than Titanium.

Conclusion: Stress generated in all constituents of the system was not significantly influenced by the bar's material. In cases without abutments, the use of a framework in Zirconia or Cobalt-Chromium exhibits biomechanical behavior similar to that of a Titanium bar. The prosthesis does not transmit the load identically through all the implants, but these differences were not significant.

Keywords: Cobalt-Chromium, Finite element analysis, Implant, Titanium, Zirconia.

Introduction

Implant dentistry plays a crucial role in restoring the normal function and aesthetics of patients, regardless of oral health conditions. Dental implants, defined as prosthetic devices made of alloplastic materials, provide support for fixed or removable dental prostheses. Through advancements in research, diagnostic tools, and materials, predictable success in implant dentistry is now achievable. The biocompatibility of biomaterials used is essential, with surface properties playing a key role. The interplay between biomaterials and biomechanics is vital for successful implant placement and tissue response. Careful evaluation of material properties and design optimization ensures optimal function and tissue compatibility in oral–maxillofacial reconstruction.[1]

The most frequently used materials for implant-supported frameworks are metal alloys. Pure metals such as gold and platinum foil do exist in dentistry, but alloys—i.e., mixtures of two or more metals, or one or more metals with a non-metal—are by far more common. To reduce costs, a number of alternatives to gold have been presented, including high-noble as well as base-metal alloys and titanium, both commercially pure (CP) and titanium alloys.[2]

In dentistry, cobalt–chrome alloys have been used since 1929, mainly for frameworks in removable partial dentures but, in recent decades, also in resin-bonded partial prostheses.[3] Their corrosion resistance is regarded as excellent due to the adherent layer of chromium-based oxides on the surface that creates a passivating effect. Minor elements are generally added to improve castability, handling, and mechanical properties.

For example, carbon affects ductility, hardness, and strength; however, excessive carbon decreases ductility and increases brittleness and the risk of fracture. In addition, tungsten helps increase corrosion resistance. Cobalt–chrome alloys have the highest melting ranges of all casting alloys apart from titanium alloys, and laboratory manipulation such as casting, adjustment, and polishing is difficult and time-consuming.[4]

Metallic alloys have higher tensile strength (>300 MPa) and elastic modulus (>80,000 MPa), which are sufficient to prevent deformation. Since the early 1950s, titanium metal has been used in numerous industrial processes. Titanium is attractive because of its low specific weight, high strength-to-weight ratio, and good resistance to fatigue and corrosion. In dentistry, it was initially used to fabricate dental implants because of its biocompatibility, while prosthetic implant-based infrastructures were initially made of precious metals. However, with the rising price of gold and the occurrence of allergic reactions to some nickel–chromium and other base-metal alloys, economically feasible alloys with reduced risks to patients

were sought. Hence, titanium implants are considered the gold standard and are widely used in implant dentistry. Corrosion resistance, biocompatibility, low cost, and good mechanical properties make titanium a viable material for the fabrication of prosthetic infrastructures on implants.[5-7]

The main limitation of metallic alloys is their dark color, which may not provide satisfactory esthetic results. Allergic reactions and galvanic side effects have also been reported. Therefore, metal-free prostheses are gaining considerable attention.[8]

Zirconia implants are an alternative to titanium implants. They possess excellent mechanical properties, low bacterial surface adhesion, and are esthetically pleasing. They can withstand long-term loading; however, high concentrations of mechanical stress (e.g., in grinding cases) can cause fracture of the implant.

Nowadays, zirconia has many applications in dentistry, including root canal posts, frameworks for all-ceramic posterior restorations, implant-supported crowns and fixed dental prostheses, custom-made bars to support fixed and removable dental prostheses, implant abutments, and dental implants. However, the incidence of chipping of ceramic-veneered zirconia frameworks has increased.

Zirconia occupies a unique position among oxide ceramics due to its excellent mechanical properties. This is largely attributed to the extensive research conducted since the discovery of the transformation toughening capabilities of this material. The different polymorphic stages of zirconia are temperature-dependent: at ambient pressure, unalloyed zirconia can assume three crystallographic forms. Pure zirconia has three polymorphic (crystalline) forms: monoclinic (m, at low temperature), tetragonal (t, at intermediate temperature), and cubic (c, at high temperature). The t-to-m transformation is martensitic in nature. It is used to improve the mechanical properties of ZrO_2 ceramics and ZrO_2 particle-reinforced composites through the mechanism of transformation toughening. The t-to-m transformation occurs at around 950°C during cooling. Transformation toughening occurs because of the volume expansion (3%–4%) that accompanies the t-to-m transformation, producing a reduction in stress intensity at the crack tip and leading to dissipation of the energy of the propagating crack. Cracks become self-limiting because an advancing crack must overcome both the energy required for material transformation and the volume expansion associated with the transformed material.[9,10]

Cyclic loading during biting or chewing simulation can gradually cause degradation of the toughening mechanisms, which may ultimately lead to fracture of the zirconia framework because a toughened material could be more susceptible to rupture. Cracks can originate within the zirconia framework or close to the ceramic veneer interface and propagate to the interface.[11]

Recently, computer-assisted fabrication (CAD/CAM) systems have emerged as a popular modality. These systems have provided significant improvements in the marginal adaptation of frameworks compared with traditional laboratory procedures. Fixed dental prostheses (FDPs) fabricated using this system demonstrate greater strength with fewer internal defects than those prepared using conventional manual laboratory techniques.[12]

Nowadays, polymeric materials have gained considerable attention, including the ultra-high-performance thermoplastic polymer family known as polyaryletherketones (PAEKs). Polyetherketoneketone (PEKK) and polyetheretherketone (PEEK) are members of this family. PEKK and PEEK have similar chemical structures, with the main difference being the replacement of a flexible ether linkage with a rigid ketone group in PEKK, leading to a higher glass transition temperature (Tg) compared with PEEK. Additionally, the arrangement of the second ketone group can be controlled to affect the

material's melting point and crystallization rate. These differences have implications for additive manufacturing (AM) and influence the mechanical response, particularly in terms of shock absorbance capacity and shear compression. PEKK, being at the top of the PAEK family, exhibits approximately 80% higher compressive strength than PEEK.[13]

Due to their good mechanical properties, elastic modulus closer to native bone and dentin, inertness, non-allergenic nature, ease of availability, and reduced biofilm accumulation, polymers are being considered as substitutes for metal alloys in prosthetic framework materials. However, further studies are required to better understand their biomechanical behavior as frameworks for full-arch fixed dental prostheses.[14]

Furthermore, graphene, a carbon-based material, is enhancing the field of dental practice. It possesses very high flexural strength, excellent esthetics, and high superficial abrasion resistance. Because of these properties, it has become a potential game changer in implant dentistry. As a superstructure material, it has the potential to act as a shock absorber, which may help prevent high-impact forces on the implant body. Currently, a limited amount of research is available on the long-term effects of graphene derivatives. Therefore, further research is crucial to better understand the potential risks and ensure safety before their extensive clinical application can be considered.[15]

The present study aimed to compare the stress distribution in implant-supported mandibular prostheses using three different framework materials, namely Titanium, Zirconia, and Cobalt-Chromium, with the help of three-dimensional finite element analysis.

Materials and Method

To conduct this study, the following materials and methodology were used:

1. **Computer with the following specifications:**

- Windows 10
- Intel Core i3 processor
- 64 GB RAM
- 225 GB hard disk

2. **FEA Software**

- The models were developed and analyzed using **ANSYS 2020** 3D finite element modeling software (Ansys Inc., TX, USA).
- Surface details and surface data of the models were generated using **SpaceClaim software**.
- Stress analysis was carried out using **ANSYS 2020 (USA)** software.

3. **Cone Beam Computed Tomography**

- A cadaveric mandible was scanned through computed tomography to obtain a digital file for generating the geometry of the mandibular FEA model.

4. **Dental Implant**
5. **Cadaveric Mandible**

The study was performed in the following steps:

- Generation of STL format of the mandible.
- Transfer of the STL format to ANSYS software to generate the FEA model via Space Claim software.
- Modeling of the mandible for the study.
- Modeling of implants and the Titanium framework.
- Modeling of implants and the Zirconia framework.
- Modeling of implants and the Cobalt-Chromium framework.
- Stress analysis.

3-D Finite Element (FE) Model Generation and Description

1. A CT scan of an edentulous patient's mandible was obtained.
2. Generation of STL format of the mandible

CT scan data were used to create DICOM files. The DICOM file of the mandible was then converted to an STL file using Slicer software. STL is the native file format of 3D Systems' stereolithography CAD software. STL stands for "Standard Triangle Language" or "Standard Tessellation Language." Many additional software applications support this file format.

3. The STL file was transferred to ANSYS software to generate the FEA model via Space Claim software. This solid model was used for FE meshing.
4. With the help of the STL file, a geometric model of the mandible was constructed.
5. The geometric models of the dental implant and prosthesis in the mandible were also generated in the same manner.
6. A graphic preprocessing software, ANSYS, was used for creating the geometric configuration of the mandible, nodes, and elements for finite element analysis.
7. This in vitro model closely resembled the in vivo geometry of the mandible, implant, abutment, bone–implant interface, and prosthesis.
8. The data were then imported into Solid Works software to create three-dimensional (3D) models of the mandible, implant, surrounding osseous tissue, and prosthesis as a collection of geometric structural elements interconnected at a finite number of nodal points.
9. The finite element model was created according to the requirements of the study.
10. The assembled finite element model of the inserted implants in bone was then imported into ANSYS software for analysis.
11. The process of converting the geometric model into a finite element model, called meshing, was performed.
12. The finite element model consisted of nodes and elements.
13. The material properties of the implant, bone, and prosthetic materials were entered during the pre-processing stage.
14. The applied force and boundary conditions were introduced during the solution stage.
15. The models were solved in the solving stage.
16. Post-processing of the results and capturing the Von Mises stress contours of each individual section in the system were performed.

3-D Finite Element (FE) Model Generation

To enhance accuracy and realism, a three-dimensional (3D) model was created for the study, as two-dimensional models may oversimplify real-life conditions. The process involved generating a 3D mandible geometry and modeling implants and superstructures using Solid Works software. All materials were assumed to be isotropic, homogeneous, and linearly elastic. The models were meshed and analyzed using ANSYS Workbench (ANSYS 2020, Inc., USA). Additionally, a 3D finite bone model was developed using Space Claim software.

This comprehensive approach resulted in the creation of three models, providing a more detailed and realistic representation for analysis. The models received four implants, where two straight implants were placed bilaterally in the first mandibular molar region and two straight implants were placed in the canine region (Fig. 1).

The study involved creating Universal Castable Long Abutment (UCLA) components tailored to individual implant heights and attaching them to a standard framework model. Retaining screws were positioned accordingly. The bar was set at 6 mm height from the bone surface, with 10 mm lever arms on each side. Screw

orifices were designed for structural strength simulation, and two 2-mm diameter circles were added for load standardization.

All components were individually modeled with different physical properties (Tables 1, 2, and 3) and then assembled (Fig. 2). The entire assembly was exported for analysis with ANSYS Workbench (ANSYS 2020, Inc., USA) through a bidirectionally interpretable translated system called Initial Graphics Exchange Specification (IGES).

An axial load of 200 N was applied bilaterally in the posterior superior region in the direction of the bone (Fig. 3). After application of the force, the magnitudes were analyzed using ANSYS Workbench (ANSYS 2020, Inc., USA), a 3D finite element analysis program.

An assessment of stress at the bone–implant interface was performed using Von Mises stress values. A color scale with stress values was used to quantitatively evaluate the stress distribution at the bone and implant interface. The stress scale ranged from 0 MPa (blue) to the highest stress values (red). Red indicated areas with the highest stress, whereas blue indicated areas with the lowest stress.

Material Properties

Homogeneous: This term implies that the material properties were the same throughout the entire structure.

Isotropy: This term implies that the material properties were identical in all directions.

Linear Elasticity: This term implies that the deformation or strain of the structure was proportional to the applied force and independent of the strain rate.

Assumptions

The program used several assumptions regarding the mechanical properties of the simulated structures.

- All materials used in the model were assumed to be homogeneous, isotropic, and linearly elastic.
- Ideal 100% osseointegration at the interface between the bone and implant was assumed in this study.
- Since the literature often provides different values for the elastic properties of the same material, average values were selected for this study.

Elements and Nodes

The models were meshed using tetrahedral ten-noded elements.

Stress Analysis

Constraints and Loads

The entire assembly was exported for analysis with ANSYS Workbench (ANSYS 2020, Inc., USA). The simulated force consisted of a 200 N axial (vertical) load applied bilaterally over the posterior superior region, ensuring movement restriction only along the Z-axis.

After the application of force, the magnitudes were analyzed using ANSYS Workbench (ANSYS 2020, Inc., USA), a 3D finite element analysis program. The influence of different framework materials (Titanium, Zirconia, and Cobalt-Chromium) on stress distribution over bone tissue-simulating material was evaluated using Von Mises stress and deformation values.

A color scale with stress values was used to quantitatively evaluate stress and deformation at the bone–implant interface. The scale ranged from 0 MPa (blue) to the highest values (red). Red indicated areas with the highest stress and deformation, whereas blue indicated areas with the lowest stress and deformation.

Results

A color scale showing Von Mises stress distribution was used to quantitatively evaluate stress distribution in the implant-supported mandibular prostheses. The scale ranged from lowest stress (blue) to highest stress (red). Red indicated areas with the highest stress loads, while blue indicated areas with the lowest stress loads.

On comparing Von Mises stress values on the implant under an axial load of 200 N on Titanium, Zirconia, and Cobalt-Chromium frameworks, the value was observed to be 94.194 for all three frameworks (Figs. 4a, 5a, and 6a).

The maximum Von Mises stress values on the implant screw with an axial force of 200 N applied bilaterally in the posterior region were observed to be 36.59 in the Zirconia and Cobalt-Chromium frameworks (Figs. 5b and 6b), whereas the value was 23.843 in the Titanium framework (Fig. 4b).

The maximum Von Mises stress values on the metal structure with an axial force of 200 N applied bilaterally in the posterior region were observed to be 94.194 in the Titanium, Zirconia, and Cobalt-Chromium frameworks (Figs. 4c, 5c, and 6c).

The maximum Von Mises stress on cortical bone with an axial force of 200 N applied bilaterally in the posterior region was 23.843 in the Titanium framework (Fig. 4d), 23.159 in the Zirconia framework (Fig. 5d), and 23.159 in the Cobalt-Chromium framework (Fig. 6d).

The maximum Von Mises stress on cancellous bone with an axial force of 200 N applied bilaterally in the posterior region was 14.288 in the Titanium framework (Fig. 4e), 11.092 in the Zirconia framework (Fig. 5e), and 11.091 in the Cobalt-Chromium framework (Fig. 6e).

Discussion

The emergence of edentulism, which can be multifactorial and include variables such as poor oral hygiene, dental caries, and periodontal disease, is a prevalent dental problem in older individuals. Patients with terminal, non-restorable dentition may experience complete or partial edentulism. The edentulous state has been found to adversely affect oral health and overall quality of life. Clinicians face an increasing demand to provide effective treatment solutions as life expectancy continues to increase, along with the need to fabricate prostheses that replace natural teeth while ensuring maximum patient satisfaction and improved quality of life.[16]

With the advancement of civilization and the development of biological, chemical, and physical sciences, there has been a gradual but steady increase in both the quantity and quality of materials used for dental implants. The ideal material should be biologically compatible, readily available, reasonably inexpensive, and easy to manipulate in order to develop prostheses that are both functionally effective and esthetically pleasing.[17]

The credit for the origin and evolution of modern bio-implants is attributed to pioneers such as Harold Ridley, Paul Winchell, Per-Ingvar Brånemark, Otto Wichterle, John Charnley, and others. Their laboratory investigations were initially tested on animals, eventually leading to the development of advanced biomaterials that could be successfully accepted by the human body.[18]

A wide range of materials are available for the fabrication of prosthetic infrastructures. Metallic alloys possess high tensile strength and elastic modulus, which are sufficient to prevent deformation.

Simamoto Júnior et al.[7] demonstrated that titanium implants are considered the gold standard in implant dentistry. Corrosion resistance, biocompatibility, low cost, and good mechanical properties make titanium a viable material for the fabrication of prosthetic infrastructures on implants. However, due to its relatively unsatisfactory esthetic outcomes, metal-free prostheses have gained increasing attention.

Takaba et al.[19] demonstrated that zirconia implants can serve as an alternative to titanium implants. They possess excellent mechanical properties, low bacterial surface adhesion, and superior esthetic characteristics.

de France et al.[20] reported that despite the variety of techniques and materials available for fabricating implant-supported frameworks, no single combination currently provides standardized results, reduced processing time, low cost, and an accurate fit simultaneously. The use of CAD/CAM technology may help reduce or eliminate some of these issues. Although CAD/CAM has been shown to be a simpler and less time-consuming technique with improved accuracy, some studies have reported a higher incidence of misfit with CAD/CAM-fabricated frameworks compared with conventionally fabricated frameworks.

The present study used the finite element method to compare stress distribution in implant-supported mandibular prostheses using Titanium, Zirconia, and Cobalt-Chromium framework materials. Finite element analysis, originally developed to solve engineering problems, is now widely used in implant biomechanics to improve implant design and prosthetic planning. While computer modeling provides several advantages for simulating the complexity of clinical conditions, FEA is also sensitive to the assumptions made regarding model parameters such as material properties, loading conditions, and boundary constraints.

In comparative analyses, complex clinical realities are often simplified, assuming that proportions and relative effects adequately represent actual conditions. In the present study, the mandible was modeled, and the shape of the bone was simplified into a rectangular block to facilitate modeling of an equal amount of bone for the three types of frameworks, namely Titanium, Zirconia, and Cobalt-Chromium. One advantage of small and simplified models is that they allow finer meshing with hexahedral elements. Thus, in the present study, the mandible with an extremely fine mesh around the implants was modelled.[21]

In the present study, three-dimensional finite element analysis was used to compare stress distribution in implant-supported mandibular prostheses fabricated using Titanium, Zirconia, and Cobalt-Chromium framework materials.

The results demonstrated that the maximum stress generated in all components of the system was not significantly influenced by the framework material. This suggests that, in cases without abutments, the use of Zirconia or Cobalt-Chromium frameworks exhibits biomechanical behavior similar to that of a Titanium bar.

Similar findings were reported by Hulterström M et al. (1991)[21] in a preliminary report in which 66 patients received implant-supported fixed prostheses with Cobalt-Chromium as the framework material. No significant differences related to framework material were observed among the patients.

However, although Cobalt-Chromium alloys have been used for implant-supported frameworks for many years, studies evaluating their long-term clinical performance remain relatively limited.

Gomes et al. (2011)[22] reported similar results in an FEA study in which the effect of different material combinations on stress distribution within metal–ceramic and all-ceramic single implant-supported prostheses was evaluated. The authors concluded that the use of different materials to fabricate a superstructure for a single implant-supported prosthesis did not significantly affect stress distribution in the supporting bone.

Bankoglu Gungor M et al. (2016)[8] conducted a three-dimensional FEA evaluating stress distribution in zirconia and titanium implant-supported prostheses and reported that prosthetic materials did not significantly alter stress distribution in bone.

Similar observations were reported by Tribst et al. (2017)[23], who demonstrated that the biomechanical

behavior of zirconia frameworks was comparable to that of titanium bars.

The findings of Rammelsberg et al. (2020)[24] were also consistent with the present study, reporting that the material used for fixed dental prostheses did not significantly influence prosthesis failure.

In the present FEA study, the maximum stress on the implant screw was found to be higher in Zirconia and Cobalt-Chromium frameworks compared with the Titanium framework under an axial load of 200 N. Similar observations were reported by Rubo and Souza (2008)[25] in their FEA study, concluding that the more rigid the structure, the more uniform the stress dissipation and the less damage caused to fastening screws due to reduced bending of the metal structure.

Tribst et al. (2017)[23] also reported that titanium, having an elastic modulus similar to that of the screw, allows stress transmission between them as a single body with less damage to the implant. In contrast, zirconia, due to the rigidity associated with its crystalline structure, tended to cause greater stress concentration in the prosthetic connection and relatively less stress in the screw.

In the present study, the maximum stress distribution in cortical bone was greater than that in cancellous bone. Saber F.S. et al. (2015)[26] also reported that maximum stresses occurred in cortical bone rather than in the underlying cancellous bone, attributing this to the higher modulus of elasticity of cortical bone, which results in greater stress concentration.

Deste G et al. (2020)[27] reported similar results in an FEA study evaluating the effects of All-on-4 implant designs in the mandible on implants and surrounding bone.

Comparable results were reported by Dogan D.O. et al. (2012)[28] in a three-dimensional FEA evaluating the All-on-4 concept and alternative implant designs, where maximum stress values were significantly higher around the cortical bone of distal implants compared with trabecular bone.

The results reported by Mahantshetty M et al. (2021)[29] were also consistent with the findings of the present study.

Sirandoni D et al. (2019)[30] reported in an FEA study that PEEK and PMMA demonstrated the highest deformation values. Conversely, stresses in cortical bone remained within physiologic limits in Ti, ZrO_2, and Co-Cr frameworks. The authors concluded that Ti, Co-Cr, and ZrO_2 frameworks demonstrated the most promising biomechanical behavior.

Lee et al. (2017)[31] compared polyetherketoneketone (PEKK) with different framework materials for implant-supported prostheses using FEA and concluded that frameworks with a lower elastic modulus (PEKK) decreased stress within the framework itself; however, they transferred greater stress to the suprastructures of the prosthesis. Observations in the present study confirm that resilient implant-supported frameworks have limited shock-absorbing properties in some regions, whereas rigid materials demonstrate more favorable stress distribution and improved structural safety for prosthetic components.

Desai S.R et al. (2023)[32] demonstrated through FEA that graphene exhibited better stress-bearing capacity compared with titanium frameworks, although both materials were considered reliable options as framework materials in implant-supported full-arch prostheses.

The limitations of the present study include the fact that Finite Element Analysis (FEA) is a mathematical in vitro model that may not completely replicate clinical conditions. Assumptions of linear elasticity and material homogeneity were made, which may affect the accuracy of the calculated stress values. Additionally, the use of

static loading conditions may not accurately reflect the complex dynamic forces present in the oral cavity. Therefore, future research combining three-dimensional FEA with long-term clinical evaluation is necessary to achieve a more comprehensive understanding of stress distribution in implant-supported prostheses.

Conclusion

A three-dimensional finite element analysis was conducted to compare the stress distribution in implant-supported mandibular prostheses using Titanium, Zirconia, and Cobalt-Chromium framework materials. For this study, a three-dimensional geometry of the edentulous mandible, comprising both cortical and cancellous bone, was generated from computed tomography scans using Solid Works software. Three models incorporating Titanium, Zirconia, and Cobalt-Chromium framework materials were developed. An axial load of 200 N was applied bilaterally to the posterior region, and the resulting stress patterns were evaluated.

Under a 200 N axial load, the maximum stress values observed on the implant and the metal structure were similar for all three framework materials. Therefore, it was observed that, in cases without abutments, the use of frameworks made of Zirconia or Cobalt-Chromium exhibits biomechanical behavior comparable to that of a Titanium bar.

Within the limitations of this study, the following conclusions were drawn:

1. Stress generated in all constituents of the system was not significantly influenced by the bar's material.
2. In cases without abutments, frameworks made of Zirconia or Cobalt-Chromium exhibit biomechanical behavior similar to that of a Titanium bar.
3. The prosthesis does not transmit the load identically through all the implants; however, these differences were not significant.

Furthermore, considering the scope of the study, the limitations identified highlight the need for further investigations correlating 3D finite element analysis findings with biological clinical conditions.

References

1. Misch CE. Dental implant prosthetics. 3rd ed. St. Louis: Elsevier; 2015.
2. Anusavice KJ, Gascone P. Dental casting and soldering alloys. In: Anusavice KJ, editor. Phillips' science of dental materials. St. Louis: Elsevier; 2003.
3. Council on Dental Materials, Instruments, and Equipment. Report on base metal alloys for crown and bridge applications: benefits and risks. J Am Dent Assoc. 1985;111:479–83.
4. McCabe JF. Applied dental materials. London: Blackwell; 1990.
5. Gonzalez J. The evolution of dental materials for hybrid prosthesis. Open Dent J. 2014;8:85–94.
6. Ferreira MB, Barão VA, Faverani LP, Hipólito AC, Assunção WG. The role of superstructure material on stress distribution in mandibular full-arch implant-supported fixed dentures: a CT-based 3D finite element analysis. Mater Sci Eng C Mater Biol Appl. 2014;35:92–9.
7. Simamoto Júnior PC, Resende Novais V, Rodrigues Machado A, Soares CJ, Araújo Raposo LH. Effect of joint design and welding type on the flexural strength and weld penetration of Ti-6Al-4V alloy bars. J Prosthet Dent. 2015;113:467–74.
8. Bankoglu Güngör M, Yilmaz H. Evaluation of stress distributions occurring on zirconia and titanium implant-supported prostheses: a three-dimensional finite element analysis. J Prosthet Dent. 2016; 116:346–55.

9. Garvie RC, Hannink RH, Pascoe RT. Ceramic steel? Nature. 1975;258:703–4.
10. Subbarao EC. Zirconia—an overview. In: Heuer AH, Hobbs LW, editors. Science and technology of zirconia. Columbus (OH): The American Ceramic Society; 1981. p. 1–24.
11. Studart AR, Filser F, Kocher P, Lüthy H, Gauckler LJ. Cyclic fatigue in water of veneer-framework composites for all-ceramic dental bridges. Dent Mater. 2007;23:177–85.
12. Suarez M, Villaumbrosia PG, Lozano JFL. Comparison of the marginal fit of Procera AllCeram crowns with two finish lines. Int J Prosthodont. 2003;16:229–32.
13. Rauch A, Hahnel S, Günther E, Bidmon W, Schierz O. Tooth-colored CAD/CAM materials for application in 3-unit fixed dental prostheses in the molar area: an illustrated clinical comparison. Materials (Basel). 2020;13:5588.
14. Villefort RF, Diamantino PJS, Zeidler SLVV, Borges ALS, Silva-Concílio LR, Saavedra GDFA, Tribst JPM. Mechanical response of PEKK and PEEK as frameworks for implant-supported full-arch fixed dental prostheses: a 3D finite element analysis. Eur J Dent. 2022;16:115–21.
15. Dawson JH, Hyde B, Hurst M, Harris BT, Lin WS. Polyetherketoneketone (PEKK), a framework material for complete fixed and removable dental prostheses: a clinical report. J Prosthet Dent. 2018;119:867–72.
16. Jensen OT, Adams MW, Cottam JR, Parel SM, Phillips WR. Treatment with mandibular V-4. J Oral Maxillofac Surg. 2009;67:90–97.
17. Huebsch N, Mooney DJ. Inspiration and application in the evolution of biomaterials. Nature. 2009;462:426–32.
18. Manivasagam G, Dhinasekaran D, Rajamanickam A. Biomedical implants: corrosion and its prevention – a review. Recent Pat Corros Sci. 2010;2:40–54.
19. Takaba M, Tanaka S, Ishiura Y, Baba K. Implant-supported fixed dental prostheses with CAD/CAM-fabricated porcelain crown and zirconia-based framework. J Prosthodont. 2013;22:402–7.
20. de França DG, Morais MH, das Neves FD, Barbosa GA. Influence of CAD/CAM on the fit accuracy of implant-supported zirconia and cobalt-chromium fixed dental prostheses. J Prosthet Dent. 2015;113:22–8.
21. Hulterström M, Nilsson U. Cobalt-chromium as a framework material in implant-supported fixed prostheses: a preliminary report. Int J Oral Maxillofac Implants. 1991;6:475–80.
22. Gomes EA, Barão VA, Rocha EP, de Almeida EO, Assunção WG. Effect of different material combinations on stress distribution in implant-supported prostheses. Int J Oral Maxillofac Implants. 2011;26:1202–10.
23. Tribst JPM, de Morais DC, Alonso AA, Piva AMOD, Borges ALS. Comparative three-dimensional finite element analysis of implant-supported fixed complete arch mandibular prostheses in two materials. J Indian Prosthodont Soc. 2017;17:255–60.
24. Rammelsberg P, Meyer A, Lorenzo-Bermejo J, Kappel S, Zenthöfer A. Long-term chipping and failure rates of implant-supported and combined tooth–implant-supported metal–ceramic and ceramic fixed dental prostheses: a cohort study. J Prosthet Dent. 2021;126:196–203.
25. Rubo JH, Souza EA. Finite element analysis of stress in bone adjacent to dental implants. J Oral Implantol. 2008;34:248–55.

26. Saleh Saber F, Ghasemi S, Koodaryan R, Babaloo A, Abolfazli N. Comparison of stress distribution with different implant numbers and inclination angles in All-on-Four and conventional methods in maxilla: a finite element analysis. J Dent Res Dent Clin Dent Prospects. 2015;9:246–53.
27. Deste G, Durkan R. Effects of All-on-Four implant designs in mandible on implants and the surrounding bone: a 3D finite element analysis. Niger J Clin Pract. 2020;23:456–63.
28. Özdemir Doğan D, Polat NT, Polat S, Şeker E, Gül EB. Evaluation of the "All-on-Four" concept and alternative designs with a 3D finite element analysis method. Clin Implant Dent Relat Res. 2014;16:501–10.
29. Mahantshetty M, Thumati P, Ayinala M. Analysis of stress distribution around angulated and parallel placed implants based on the All-on-4 concept and four implants placed parallel within the interforaminal distance in an edentulous mandible: an in vitro three-dimensional finite element analysis. J Dent Implants. 2021;11:44–52.
30. Sirandoni D, Leal E, Weber B, Noritomi PY, Fuentes R, Borie E. Effect of different framework materials in implant-supported fixed mandibular prostheses: a finite element analysis. Int J Oral Maxillofac Implants. 2019;34:e107–14.
31. Lee KS, Shin SW, Lee SP, Kim JE, Kim JH, Lee JY. Comparative evaluation of a four-implant-supported polyetherketoneketone framework prosthesis: a three-dimensional finite element analysis based on cone beam computed tomography and computer-aided design. Int J Prosthodont. 2017;30:581–5.
32. Desai SR, Koulgikar KD, Alqhtani NR, Alqahtani AR, Alqahtani AS, Alenazi A, et al. Three-dimensional FEA analysis of stress distribution on titanium and graphene frameworks supported by 3- or 6-implant models. Biomimetics (Basel). 2023;8:15.

Legend Tables, Figures and Graphs

Table 1: The properties, Young's Modulus and Poisson's ratio, of the materials used

Material	Young's Modulus(GPa)	Poisson's coefficient
Cortical bone	15	0.30
Trabecular bone	1	0.25

Table 2: Mechanical properties - Implant model

Material	Component	Young's Modulus (GPa)	Poisson's coefficient
Ti-6Al-4V alloy	Abutment and screw	107.2	0.30
	Dental implant	110	0.35

Table 3: Material properties - Prosthetic Bar

Material	Component	Young's Modulus(GPa)	Poisson's coefficient
Cr-Co alloy	Bar	218	0.33
Zirconia	Bar	200	0.31
Titanium Alloy	Bar	110	0.33

Table 4: Descriptive von Mises stress (MPa) values with axial load (200N) bilaterally on posterior region on Titanium framework.

Titanium framework	Implant	Implant screw	Metal structure	Cortical Bone	Cancellous Bone
Stress in MPa	94.194	23.843	94.194	23.843	14.288

Table 5: Descriptive von Mises stress (MPa) values with axial load (200N) bilaterally on posterior region on Zirconia framework.

Zirconia framework	Implant	Implant screw	Metal structure	Cortical Bone	Cancellous Bone
Stress in MPa	94.194	36.59	94.194	23.159	11.092

Table 6: Descriptive von Mises stress (MPa) values with axial load (200N) bilaterally on posterior region on Cobalt-Chromium framework.

Cobalt-Chromium framework	Implant	Implant screw	Metal Structure	Cortical Bone	Cancellous Bone
Stress in MPa	94.194	36.59	94.194	23.159	11.091

Table 7: Comparison of von Mises stress (MPa) values on the implant under axial load (200N) on Titanium, Zirconia and Cobalt-Chromium frameworks

Type	Von Mises Stress		
Implant	Axial Load (200N)	Axial Load (200N)	Axial Load(200N)
	Titanium framework	Zirconia framework	Cobalt-Chromium framework
	94.194	94.194	94.194

Table 8: Comparison of von Mises stress (MPa) values on the Implant screw under axial load (200N) on Titanium, Zirconia and Cobalt-Chromium frameworks

Type	Von Mises Stress		
Implant Screw	Axial Load (200N)	Axial Load (200N)	Axial Load(200N)
	Titanium framework	Zirconia framework	Cobalt-Chromium framework
	23.843	36.59	36.59

Table 9: Comparison of von Mises stress (MPa) values on the Metal Structure under axial load (200N) on Titanium, Zirconia and Cobalt-Chromium frameworks

Type	Von Mises Stress		
Metal Structure	Axial Load (200N)	Axial Load (200N)	Axial Load(200N)
	Titanium framework	Zirconia framework	Cobalt-Chromium framework
	94.194	94.194	94.194

Table 10: Comparison of von Mises stress (MPa) values on the Cortical Bone under axial load (200N) on Titanium, Zirconia and Cobalt-Chromium frameworks

Type	Von Mises Stress		
Cortical Bone	Axial Load (200N)	Axial Load (200N)	Axial Load (200N)
	Titanium Framework	Zirconia Framework	Cobalt-Chromium Framework
	23.843	23.159	23.159

Table 11: Comparison of von Mises stress (MPa) values on the Cancellous Bone under axial load (200N) on Titanium, Zirconia and Cobalt-Chromium frameworks

Type	Von Mises Stress		
Cancellous Bone	Axial Load (200N)	Axial Load (200N)	Axial Load (200N)
	Titanium Framework	Zirconia Framework	Cobalt-Chromium Framework
	14.288	11.092	11.091

Table 12: Comparison of von Mises stress (MPa) values of cortical bone, cancellous Bone, Implant, Implant screw and metal structure in Titanium, Zirconia and Cobalt-Chromium frameworks under axial load (200N).

	Titanium framework	Zirconia framework	Cobalt-Chromium framework
	Axial Load (200N)	Axial Load (200N)	Axial Load (200N)
Cortical bone	23.843	23.159	23.159
Cancellous bone	14.288	11.092	11.091
Implant	94.194	94.194	94.194
Implant screw	23.843	36.59	36.59
Metal structure	94.194	94.194	94.194

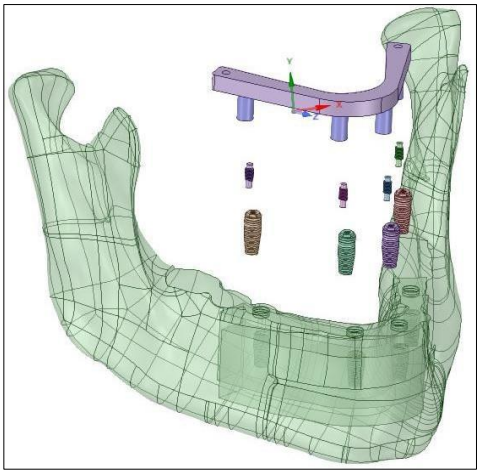

Figure 1: Modeling of different components of the model

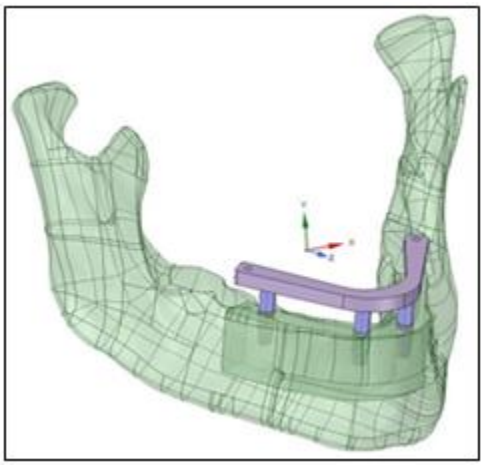

Figure 2: Assembly of different components of the model

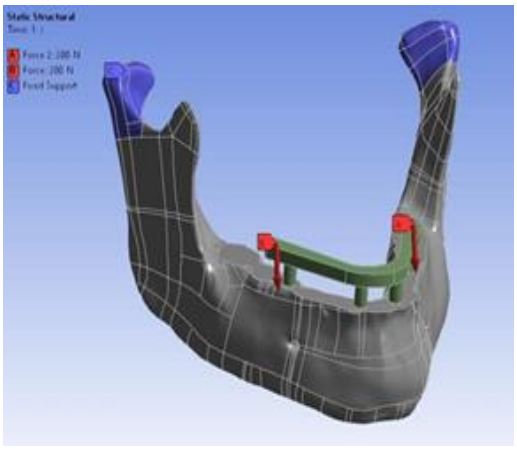

Figure 3: Application of an axial load of 200 N bilaterally at the posterior superior region in the direction of the bone

Figure 4: a, b, c, d, e

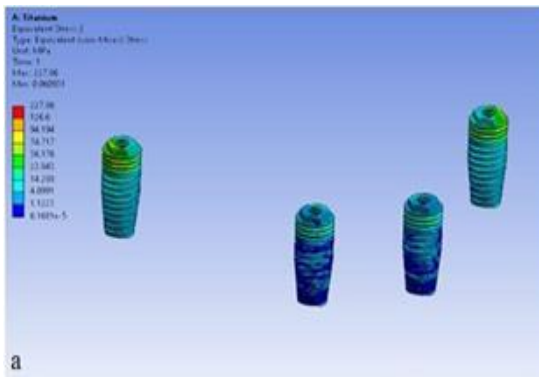

Fig. 4a: Maximum Von Mises stress on implants in the Titanium framework when loaded with an axial load of 200 N

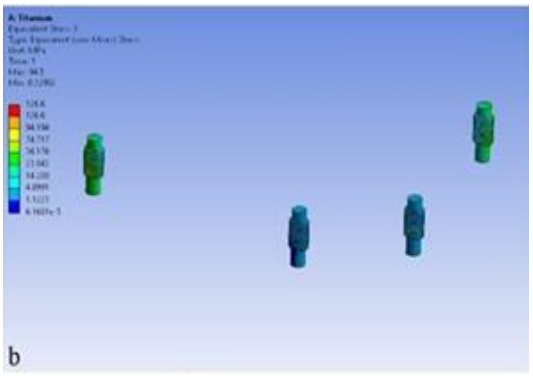

Fig. 4b: Maximum Von Mises stress on the implant screw in the Titanium framework when loaded with an axial load of 200 N

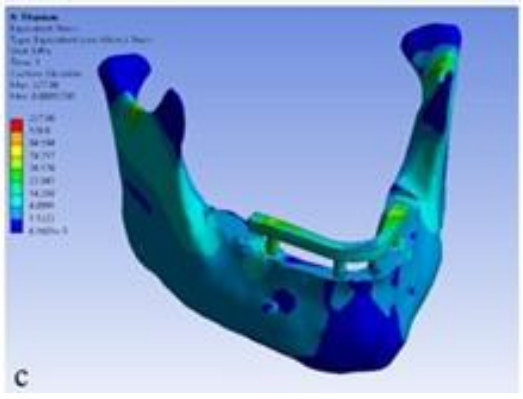

Fig. 4c: Maximum Von Mises stress on the metal structure in the Titanium framework when loaded with an axial load of 200 N

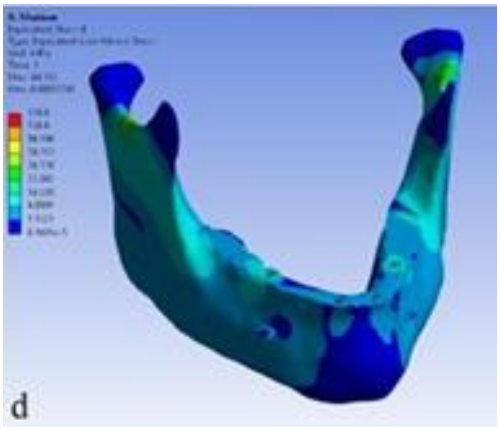

Fig. 4d: Maximum Von Mises stress on cortical bone in the Titanium framework when loaded with an axial load of 200 N

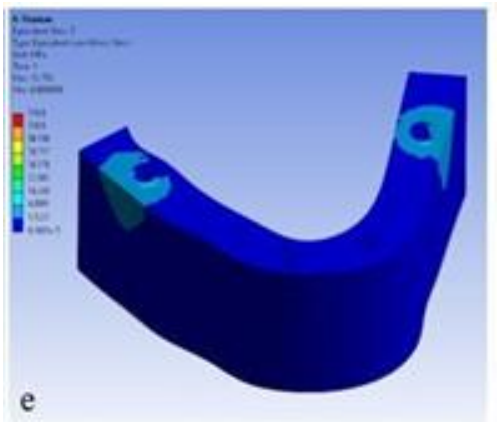

Fig. 4e: Maximum Von Mises stress on cancellous bone in the Titanium framework when loaded with an axial load of 200 N

Fig. 5 a, b, c, d, e

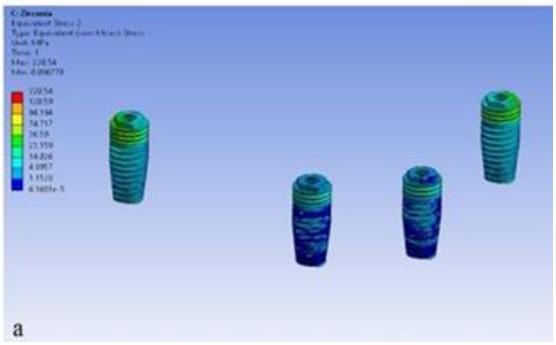

Fig. 5a: Maximum Von Mises stress on the implant in the Zirconia framework when loaded with an axial load of 200 N

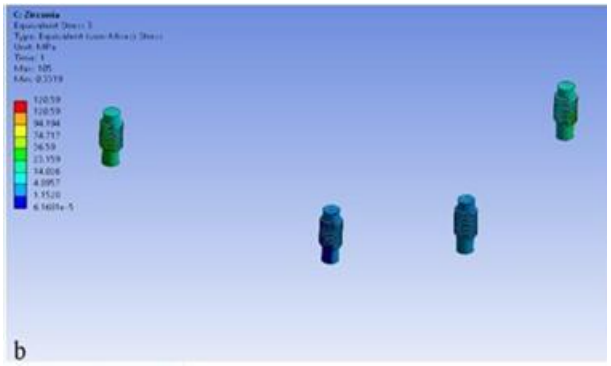

Fig. 5b: Maximum Von Mises stress on the implant screw in the Zirconia framework when loaded with an axial load of 200 N

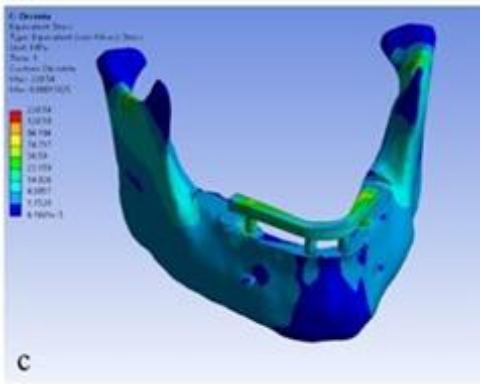

Fig. 5c: Maximum Von Mises stress on the metal structure in the Zirconia framework when loaded with an axial load of 200 N

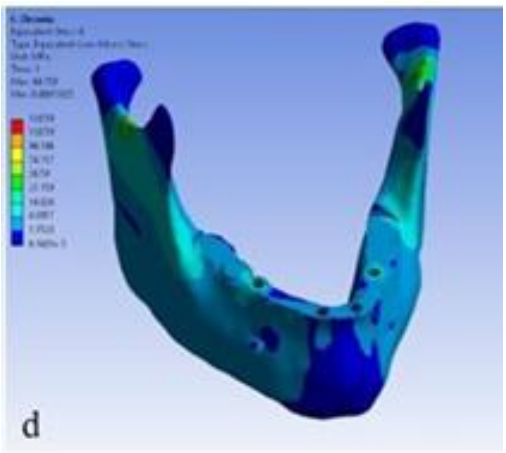

Fig. 5d: Maximum Von Mises stress on cortical bone in the Zirconia framework when loaded with an axial load of 200 N

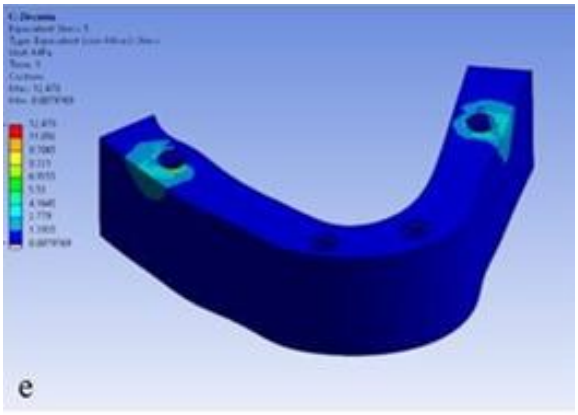

Fig. 5e: Maximum Von Mises stress on cancellous bone in the Zirconia framework when loaded with an axial load of 200 N.

Fig. 6 a, b, c, d, e

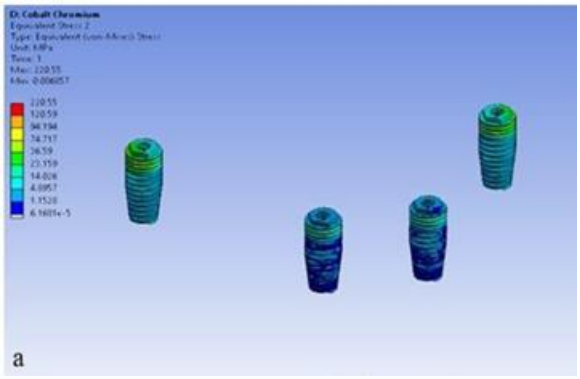

Fig. 6a: Maximum Von Mises stress on the implant in the Cobalt-Chromium framework when loaded with an axial load of 200 N.

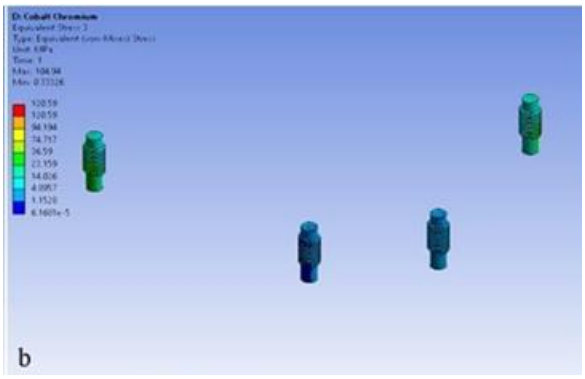

Fig. 6b: Maximum Von Mises stress on the implant screw in the Cobalt-Chromium framework when loaded with an axial load of 200 N.

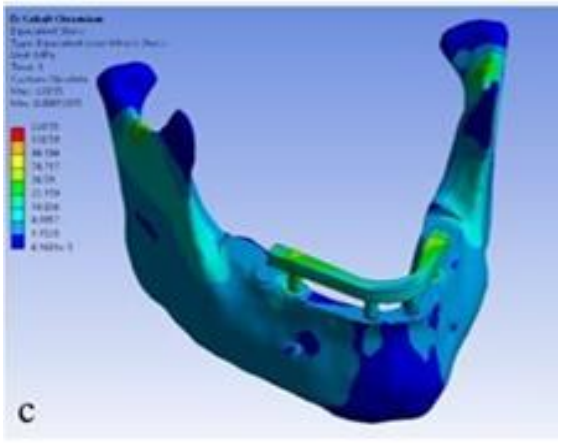

Fig. 6c: Maximum Von Mises stress on the metal structure in the Cobalt-Chromium framework when loaded with an axial load of 200 N.

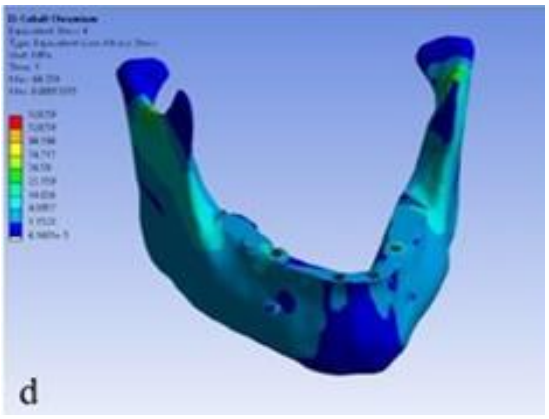

Fig. 6d: Maximum Von Mises stress on cortical bone in the Cobalt-Chromium framework when loaded with an axial load of 200 N.

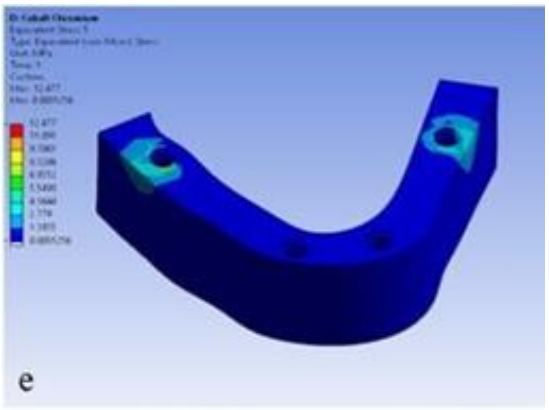

Fig. 6e: Maximum Von Mises stress on cancellous bone in the Cobalt-Chromium framework when loaded with an axial load of 200 N.

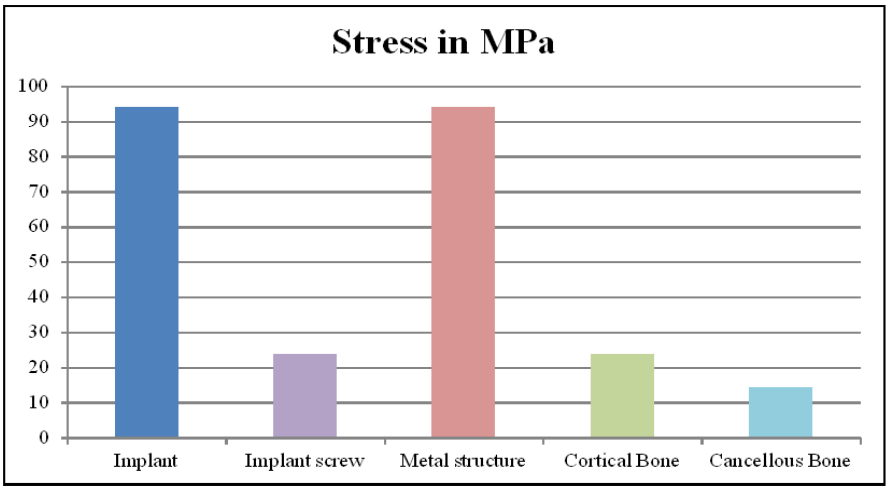

Graph 1: Descriptive Von Mises stress (MPa) values under an axial load (200 N) applied bilaterally to the posterior region on the Titanium framework.

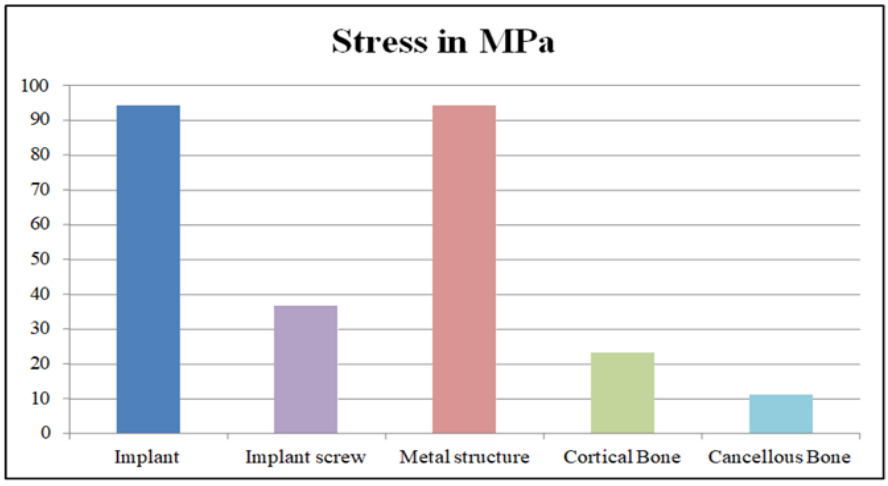

Graph 2: Descriptive Von Mises stress (MPa) values under an axial load (200 N) applied bilaterally to the posterior region on the Zirconia framework.

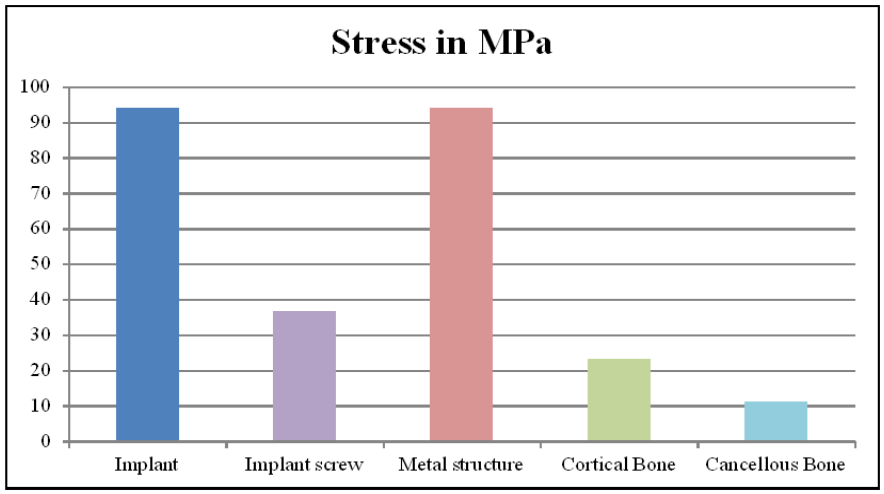

Graph 3: Descriptive Von Mises stress (MPa) values under an axial load (200 N) applied bilaterally to the posterior region on the Cobalt-Chromium framework.

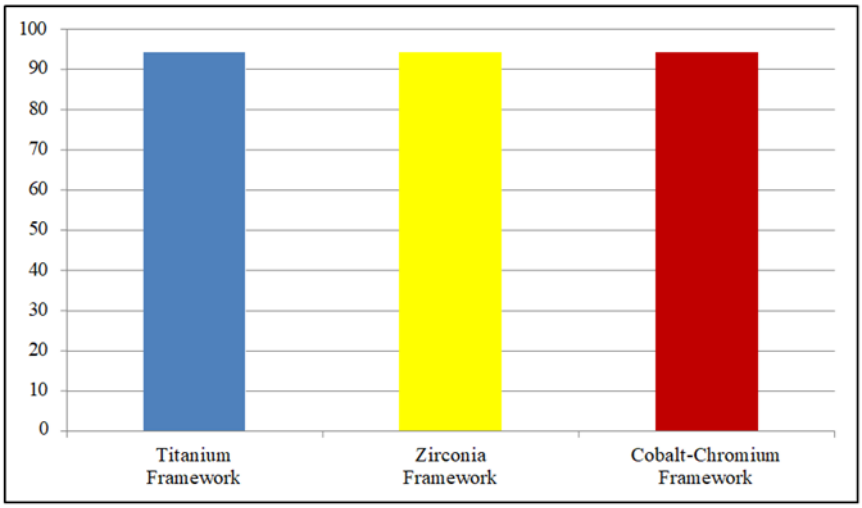

Graph 4: Comparison of Von Mises stress (MPa) values on the implant under an axial load (200 N) in Titanium, Zirconia, and Cobalt-Chromium frameworks.

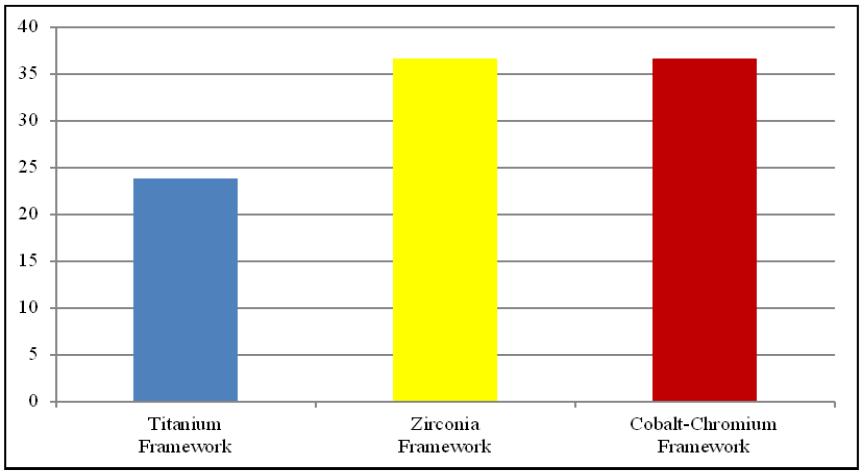

Graph 5: Comparison of Von Mises stress (MPa) values on the implant screw under an axial load (200 N) in Titanium, Zirconia, and Cobalt-Chromium frameworks.

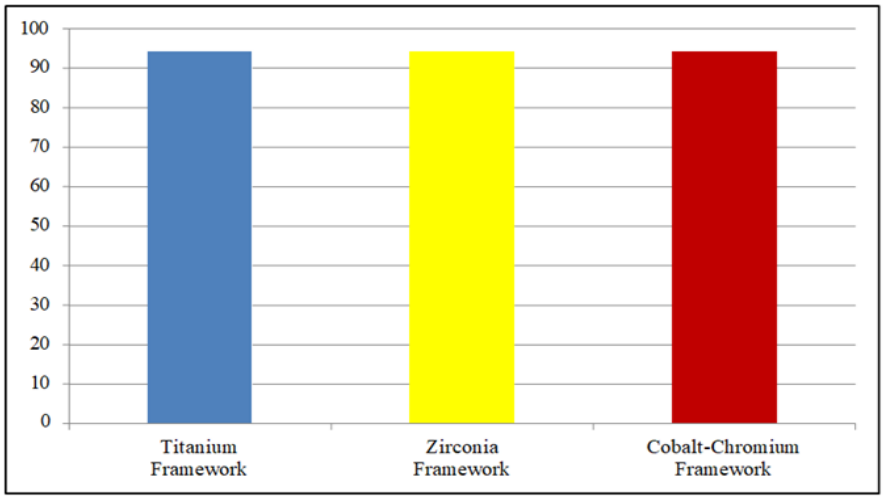

Graph 6: Comparison of Von Mises stress (MPa) values on the metal structure under an axial load (200 N) in Titanium, Zirconia, and Cobalt-Chromium frameworks

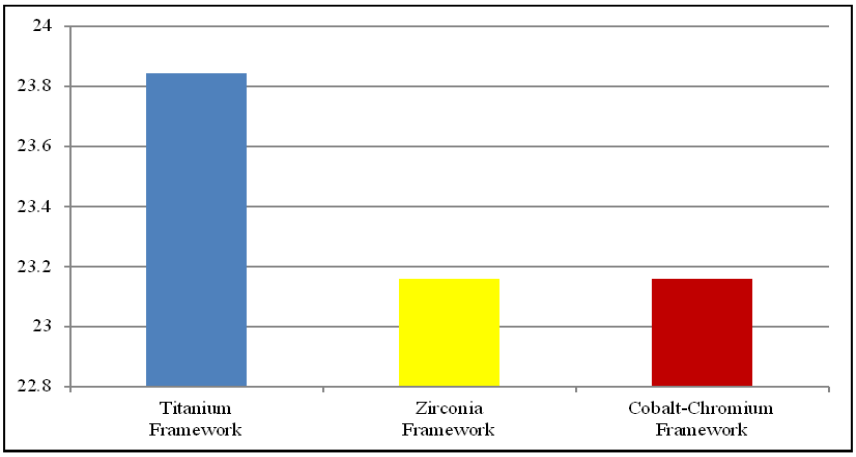

Graph 7: Comparison of von Mises stress (MPa) values on the Cortical Bone under axial load (200N) on Titanium, Zirconia and Cobalt-Chromium frameworks

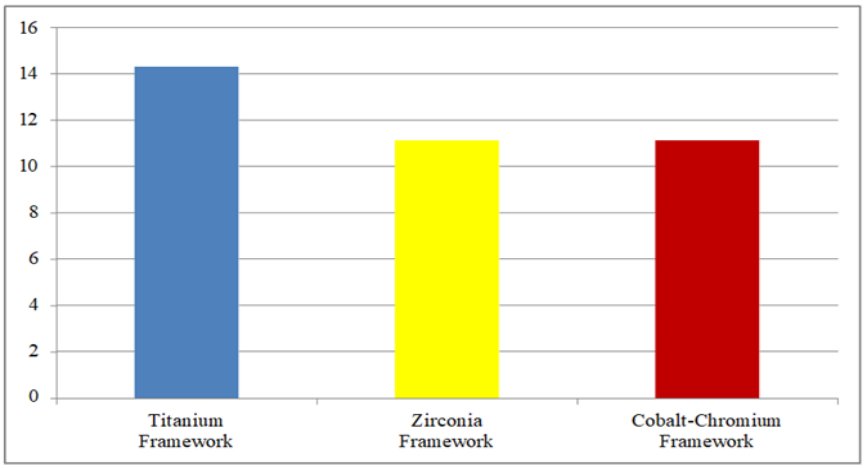

Graph 8: Comparison of von Mises stress (MPa) values on the Cancellous Bone under axial load (200N) on Titanium, Zirconia and Cobalt-Chromium frameworks

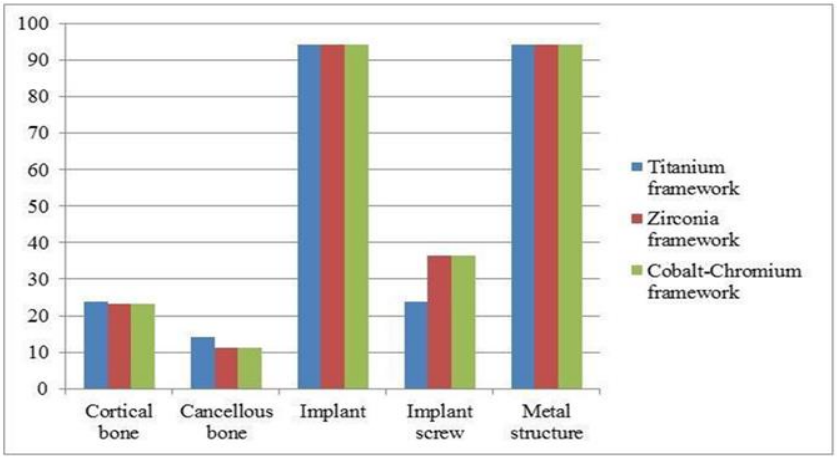

Graph 9: Comparison of von Mises stress (MPa) values of cortical bone, cancellous Bone, Implant, Implant screw and metal structure in Titanium, Zirconia and Cobalt-Chromium frameworks under axial load (200N).